Spin wave chaos in active resonant rings based on ferromagnetic films

A V Kondrashov, A B Ustinov, B A Kalinikos
Department of Physical Electronics and Technology, St.Petersburg Electrotechnical University, 5 Popov Street, St.Petersburg 197376, Russia

E-mail: kondrashov_av@yahoo.com

Abstract. Development of a microwave dynamical chaos in an active ring oscillator based on a ferromagnetic film upon a gradual increase of the ring gain has been studied. It was demonstrated that the transition of the system from steady-state to chaotic dynamics is in good agreement with the Ruelle-Takens scenario. The attractors of the dynamic system were reconstructed from the experimentally measured waveforms, and a numerical analysis of their parameters was made.

1. Introduction

Recently, a steadily increasing attention has been given to the dynamical chaos. The keen interest in this phenomenon is due to a number of its inherent properties, such as the communication confidentiality, larger information capacity, possible self-synchronization of a transmitter and receiver, etc. In this context, a study of new methods for generation of the dynamical chaos and of the process in which it appears becomes topical.

It has been demonstrated that the dynamical chaos can be generated by using bulk ferrite samples [1, 2], active resonant rings based on ferromagnetic films [3-8] or ferrite-ferroelectric multiferroic structures [9]. We stress, that transition to dynamical chaos is caused by appearance and development of nonlinear parametrical processes. For ferrite-ferroelectric structures nonlinearity of hybrid spin-electromagnetic waves have dual electric and magnetic nature [9]. In contrast to the multiferroics, nonlinear parametric processes in ferrite films are caused by only magnetic nonlinearity. In papers [1-8], the nonlinear processes developed due to either three-wave or four-wave spin wave interaction. Transition to dynamical chaos in multiferroic and ferrite structures may have similar scenario but different underlying physics. Therefore ferrite-film-based active resonant rings with single nonlinearity are of particular interest.

The goal of our study was to examine the development of chaos in active resonant rings based on ferromagnetic films under the conditions of a nonlinear only four-wave scattering of backward volume spin waves.

2. Experimental set-up

To perform an experiment, we assembled a model generator as an active ring. The block diagram of the generator is shown in figure 1. It comprised series-connected ferromagnetic delay line (1), microwave amplifier (2), adjustable attenuator (3), and directional coupler (4). The delay line was the frequency-setting element of the circuit, and the amplifier served to compensate for the loss of the

microwave signal in the delay line and attenuator. The attenuator was used to vary the ring gain. The microwave signal being generated was extracted from the ring with a directional coupler.

The delay line was fabricated from a single-crystal yttrium-iron garnet (YIG) film (5) grown by epitaxy on a gadolinium-gallium garnet substrate. The film was placed on spin-wave transducers (6) fabricated as segments of microstrip transmission lines. The 50-μm-wide and 2-mm-long transducers were short-circuited at ends. The microwave power was fed into the input transducer and extracted from the output transducer with microstrip lines (7) having a wave impedance of 50 Ohm. The YIG was 5.2 μm thick and its saturation magnetization was 1750 Gs. The film was magnetized to saturation with a dc magnetic field directed tangentially to the film plane and in parallel to the spin wave propagation direction. This orientation of the field provided excitation of the so-called backward volume spin waves in the film. The magnetization field strength of 1300 Oe was chosen so that the nonlinearity of the spin waves was only determined by four-wave interaction processes. The model generator is a resonator whose spectrum can be obtained if the attenuation is made stronger and a weak signal is introduced [10].

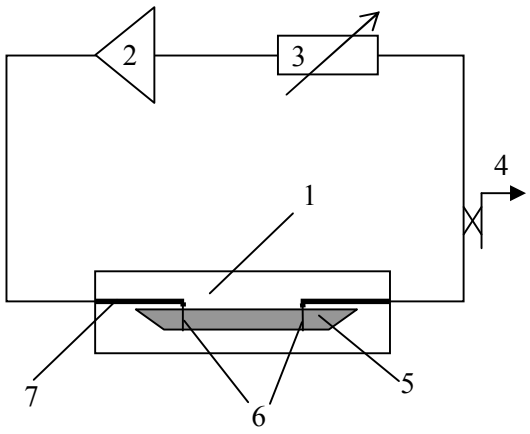

Figure 1. Block diagram of the experimental model generator.

3. Experimental results and discussion

In the course of the experiment, we gradually raised the ring gain *G*. At its certain value, the gain fully compensated for the attenuation and a self-generation of monochromatic spin waves appeared in the ring. This value of the gain was taken to be zero. Further increase in the gain resulted in a change of generation regimes. In the frequency domain, these regimes can be conditionally divided into three types; generation of a monochromatic signal, generation of a frequency comb, and generation of a dynamical chaos.

Figure 2 shows spectral characteristics (right-hand panel) and waveforms for four ring generation regimes. Figure 2(a) corresponds to the monochromatic generation mode. A single generated frequency of 5.653 GHz can be seen in the spectrum. Further increase in the gain results in that this frequency becomes unstable and breaks down into a frequency comb. In this case, generation of a sequence of nonlinear pulses, envelope solitons, was observed in the time domain. The pulses had a repetition period of 186 ns, width of 54 ns, and a carrier frequency of 5.652 GHz. At $G > 0.35$ dB, the generation of solitons was disrupted and a periodic stationary sequence of nonlinear pulses with a nonsoliton shape was generated (see figure 2(c)). With the gain raised to an even greater extent to $G =$ 0.9 dB, the signal being generated became stochastized.

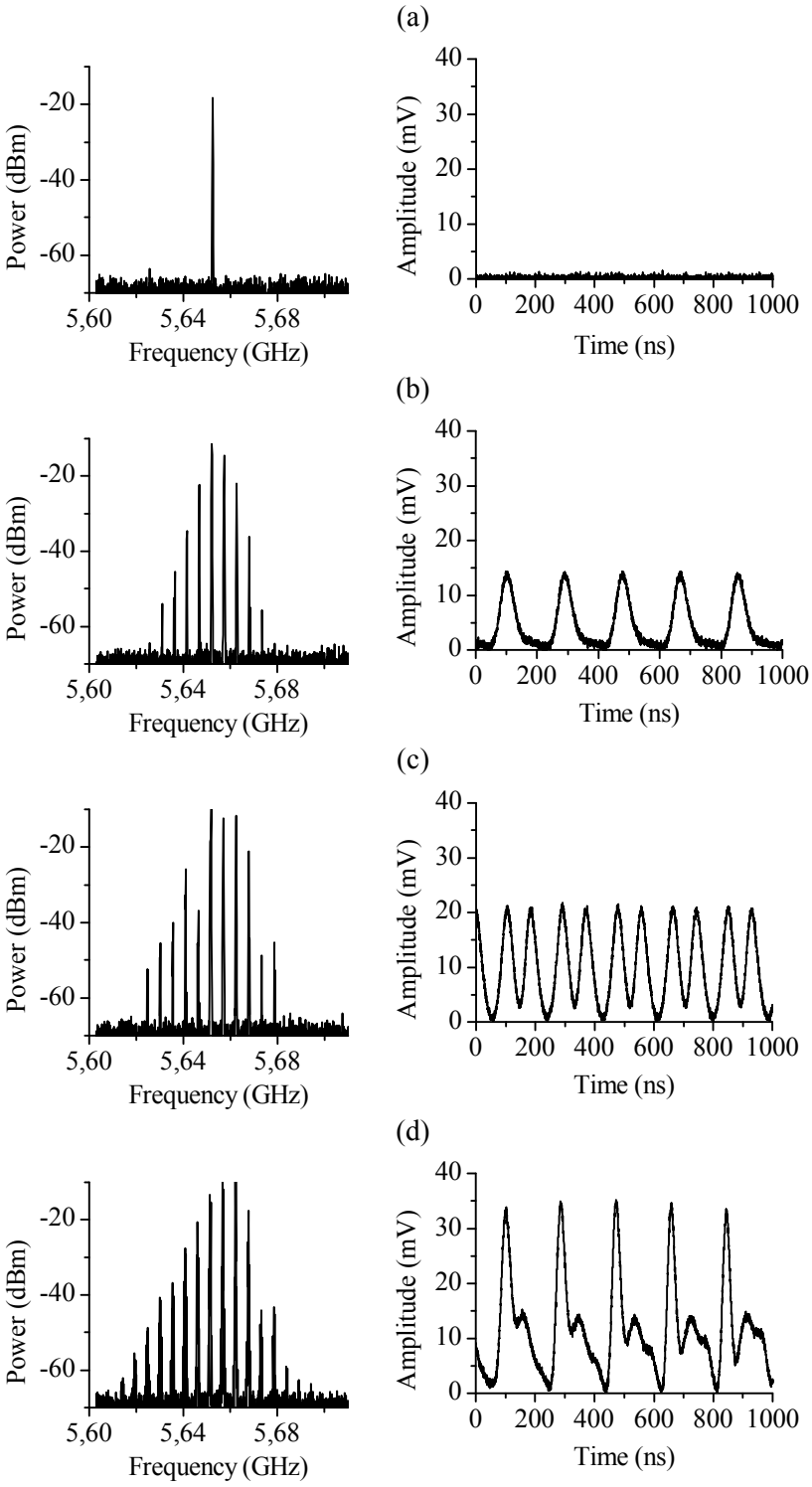

Figure 2. Spectral characteristics and waveforms for different gains G (dB): (a) 0, (b) 0.2, (c) 0.35, and (d) 1.2.

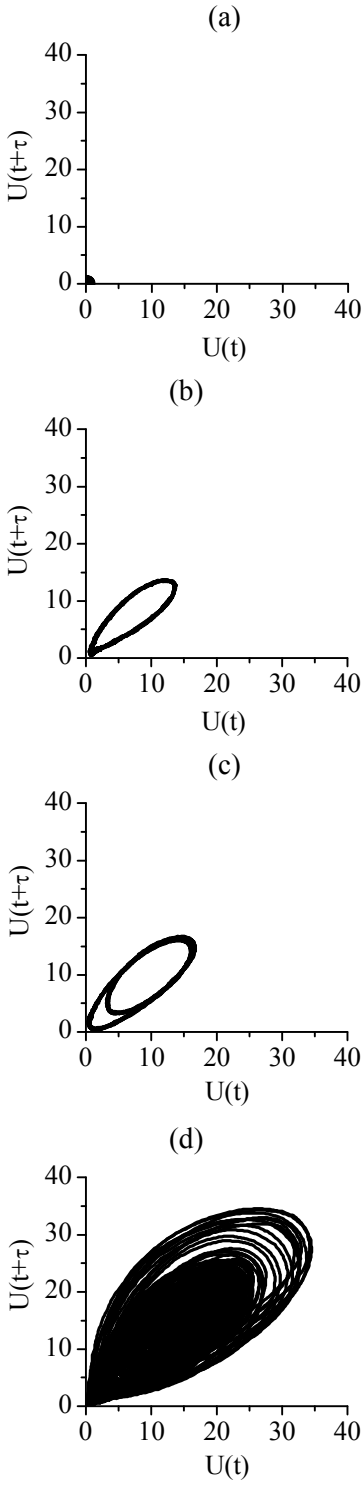

Figure 3. Attractor projections: (a) monochromatic signal, (b) envelope solitons, (c) periodic stationary pulses, and (d) dynamical chaos.

As is seen from figure 2(a) formation of bright *spin wave* solitons took place. It is due to attractive nonlinearity of backward volume spin waves propagating in tangentially magnetized YIG film. This situation is different from active rings based on multiferroic structures. The ring structure reported in [9] generates dark *spin-electromagnetic wave* solitons. Nonlinearity of the spin-electromagnetic waves (and consequently soliton properties) is controlled by electric field, that confirms different nature of nonlinear excitations.

It can be seen in figure 2 that the transition from the monochromatic generation to the chaotic type occurs via a sequence of bifurcations in which the spectrum of the microwave signal being generated is enriched in new frequencies. To further analyze the results obtained, we constructed phase portraits for each generation regime. The attractors were reconstructed by the standard time-delay method [11]. In this case, the components of the d-dimensional vector $\boldsymbol{x}(t)$ in the phase space were obtained by the time-shift of the signal $U(t)$ by a certain delay τ:

$$\boldsymbol{x}(t) = \{U(t), U(t+\tau), ..., U(t+(d-1)\tau)\}. \quad (1)$$

Figure 3 shows 2D phase portraits of the four generation modes described above. To the monochromatic signal generation mode corresponds a regular attractor, a stable point (see figure 3a). At $G > 0.2$ dB, there occurs a Hopf bifurcation corresponding to generation of a limit cycle from the stable point (see figure 3(b)). With the gain increasing further, a period-doubling bifurcation occurs (see figure 3(c)). At $G > 1.2$ dB, a strange attractor was formed (see figure 3(d)). This transition corresponds to the Ruelle-Takens scenario.

The phase portraits were used to calculate the quantitative characteristics of the signals: correlation integrals, fractal dimensions, and embedding dimensions. The calculation was carried out with the standard Grassberger-Procaccia algorithm [12]. The value of the correlation integral shows the number of pairs of points spaced by a distance l. Figure 4 demonstrates the dependence of the correlation integral on l for different attractor embedding dimensions.

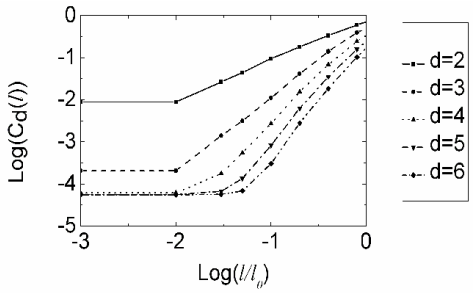

Figure 4. Curves describing the dependence of the logarithm of the correlation integral, $\log(C_d(l))$, on the logarithm $\log(l/l_0)$ for different embedding dimensions; l_0 is the a normalization constant.

Figure 5 shows how the correlation dimension depends on the attractor embedding dimension. It can be seen from the figures that, in all cases, this dimension tends to approach a constant value ("saturates") at a certain attractor embedding dimension. This value is the attractor embedding dimension and characterizes the number of degrees of freedom of the given system. At the same time, the value of the correlation dimension D_c is the fractal dimension of the attractor of the dynamic system.

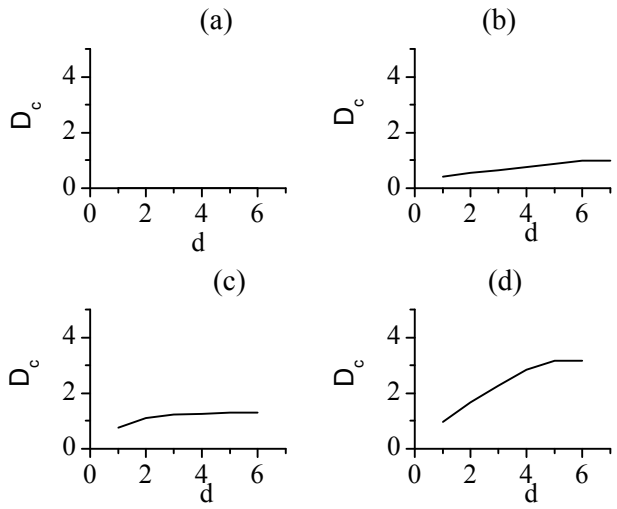

Figure 5. Correlation dimension plotted against the embedding dimension: (a) monochromatic signal, (b) envelope solitons, (c) periodic pulses, and (d) dynamical chaos.

It can be seen in figure 5(a) that the fractal dimension is 0 for the monochromatic generation mode and this value is reached already at the embedding dimension of 1. For the case of soliton generation, the fractal dimension and the embedding dimension are 1 and 6, respectively (see figure 5b). This means that the attractor is a limit cycle (see figure 3(b)).

Figure 6 shows how the fractal dimension depends on the ring gain. It can be seen in the figure that the fractal dimension grows with increasing gain. In the chaotic generation regime, the fractal dimension was 3.2. These results suggest that a dynamical chaos starts to develop in the ring at a gain G = 1.2 dB.

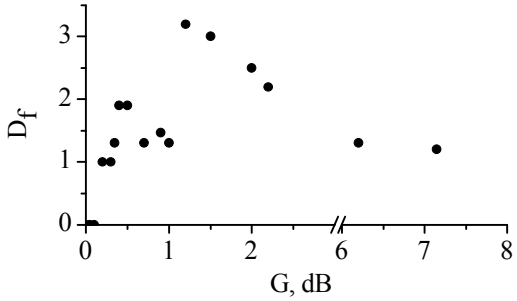

Figure 6. Dependence of the fractal dimension on the ring gain.

It is notable that, as the gain increases to more than 6, the oscillation spectrum becomes depleted. In the time domain, periodic oscillations are again observed and the fractal dimension decreases to 1.3. This transition from chaotic oscillations to those of the periodic type invites a further study.

Acknowledgement

The work was supported in part by the Russian Foundation for Basic Research and by Ministry of Education and Science of Russian Federation (Project "Goszadanie").

References

[1] Yamazaki H 1988 *J.Appl.Phys.* **64** 5391
[2] Gibson G and Jeffries C 1984 *Phys. Rev. A* **29** 811

[3] Kondrashov A V, Ustinov A B, Kalinikos B A and Benner H 2008 *Tech. Phys. Lett.* **34** 492
[4] Kondrashov A V, Ustinov A B and Kalinikos B A 2010 *Tech. Phys. Lett.* **36** 224
[5] Wang Z, Hagerstrom A, Anderson J, Tong W, Wu M, Carr L D, Eykholt R and Kalinikos B A 2011 *Phys. Rev. Lett.* **107** 114102
[6] Grishin S V, Sharaevskii Y P, Nikitov S A and Romanenko D V 2013 *IEEE Trans. on Magn.* **49** 1047
[7] Grishin S V, Golova T M, Morozova M A, Romanenko D V, Seleznev E P, Sysoev I V, Sharaevskii Y P 2015 *JETP* **121** 714
[8] Demidov V E, Kovshikov N G 1999 Technical Physics **44** 960
[9] Ustinov A B, Kondrashov A V, Nikitin A A and Kalinikos B A 2014 Appl. Phys. Lett. 104 234101
[10] Kalinikos B A, Scott M M, and Patton C E 2000 *Phys. Rev. Lett.* **84** 4697
[11] Takens F 1981 *Dynamical Systems and Turbulence, Lecture Notes in Mathematics* **898** 366
[12] Kantz H and Schreiber T 2004 *Nonlinear Time Series Analysis - 2nd edition* (Cambridge: University press)